JOURNAL OF THERMOPHYSICS AND HEAT TRANSFER
Vol. 20, No. 3, July–September 2006

Transient Natural Convective Conjugate Cooling Mechanism in Vertical Fins

I. Contreras* and C. Trevino†
Universidad Nacional Autonoma de Mexico, 04510 Mexico, D. F., Mexico
and
F. J. Higuera‡
Universidad Politécnica de Madrid, 28040 Madrid, Spain

An analysis is presented of the time-periodic conjugate free convective heat transfer from a long vertical, thermally thin fin heated from above to the surrounding fluid. The temperature at the top of the fin oscillates with a given frequency about a mean value that is higher than the temperature of the ambient fluid. The solution for very long fins depends on four nondimensional parameters: the Prandtl number of the fluid; the relative amplitude of the thermal oscillation; the Fourier number, which is the ratio of the period of the thermal oscillation to the conduction time in the fin over a length determined by the steady solution; and the ratio of this latter time to the residence time of the fluid in the boundary layer. Numerical and asymptotic results are given covering a wide region of the parametric space. A linearized version of the governing equations is worked out and shown to give oscillatory Nusselt numbers in excellent accordance with the results from the full nonlinear equations.

Nomenclature

A	=	nondimensional parameter, Eq. (4)
c	=	specific heat of fluid
Fo	=	Fourier number, Eq. (5)
G	=	nondimensional function, Eq. (34)
g	=	gravity acceleration
H	=	half-thickness of the fin
h	=	nondimensional stream function, Eq. (14)
L	=	length of the fin
L_ω	=	transient thermal penetration length, $(\alpha_w/\omega)^{1/2}$
L^*	=	steady thermal penetration length, Eq. (1)
Nu	=	Nusselt number, Eq. (2)
Nu^*	=	reduced Nusselt number, Eq. (19)
Pr	=	Prandtl number of the fluid, ν/α
Q	=	total heat flux at the top of the fin
Ra_H	=	Rayleigh number based on the half-thickness of the fin
Ra^*	=	Rayleigh number, $g\beta\Delta T L^{*3}/\alpha\nu$
s	=	ratio of L^* to L
T_0	=	mean temperature at the top of the fin
T_∞	=	temperature of the fluid far from the fin
U, V	=	nondimensional longitudinal and transverse velocity components, respectively, Eq. (6)
u, v	=	longitudinal and transverse fluid velocity components, respectively
x, y	=	Cartesian coordinates, longitudinal and transverse, respectively
Y	=	nondimensional transverse coordinate defined in Eq. (6)
α	=	thermal diffisivity of fluid
β	=	thermal expansion coefficient of fluid
γ	=	nondimensional temperature amplitude, $\Delta T/(T_0 - T_\infty)$
ΔT	=	amplitude of the temperature oscillation at the top of the fin
ε	=	aspect ratio of the fin, H/L
ζ	=	nondimensional longitudinal coordinate, Eq. (6)
$\hat{\zeta}$	=	stretched coordinate, $(\zeta - 1)\sigma_0/Fo^{1/2}$
θ	=	nondimensional temperature of fluid, Eq. (6)
θ_w	=	nondimensional temperature of the fin, Eq. (6)
λ	=	thermal conductivity of fluid
λ_w	=	thermal conductivity of the fin
ν	=	kinematic coefficient of viscosity of fluid
ξ	=	nondimensional coordinate, Eq. (14)
ρ	=	density of fluid
σ_0	=	nondimensional parameter, Eq. (6)
τ	=	nondimensional time, Eq. (6)
ϕ	=	nondimensional fluid temperature
φ	=	nondimensional temperature of the fin, Eq. (22)
Ψ_r, Ψ_i	=	real and imaginary functions, Eq. (23)
ω	=	frequency of the thermal oscillation

Subscripts

c	=	characteristic values of parameter
u	=	at the top of the fin
w	=	properties of the fin
wh	=	transverse variations of properties in the fin
ω	=	transient process
∞	=	conditions of the fluid far from the fin

I. Introduction

THE problem of the thermal coupling between natural convection and heat conduction in vertical or horizontal surfaces has been extensively studied in the heat transfer literature.[1–3] Lock and Gunn[4] analyzed a tapered isothermal short fin in a stagnant fluid with a very large Prandtl number, using a similarity formalism. The first investigation where the longitudinal heat conduction in the fin was shown to modify the thermal characteristics was carried out by Sparrow and Acharya.[5] These authors show that the heat transfer coefficient along a fin is not uniform but varies with the distance measured from its base. Kuehn et al.[6] presented a similarity solution for the conjugate free convection heat transfer from an infinitely long vertical fin at different values of Prandtl number. A similar study using an integral formalism has been published by

Received 9 December 2004; revision received 11 July 2005; accepted for publication 18 July 2005.

*Graduate Student, Facultad de Ingeniería.
†Professor, Facultad de Ciencias, Departamento de Física; ctrev@servidor.unam.mx.
‡Professor, School of Aeronautics.

Himasekhar[7] for a very long fin, whereas Sarma et al.[8] extended the formulation to the case of a heat-generating fin, assuming prescribed velocity and temperature profiles. Mobedi et al.[9] solved the conjugate conduction–natural convection heat transfer problem on a rectangular fin attached to a partially heated horizontal base for air in laminar and steady flow. Treviño et al.[10] studied the steady problem of a vertical fin heated from the top, pointing out that the most important parameter of this problem is the ratio of a thermal penetration length L^* (to be discussed in Sec. II) to the length of the fin L. They solved the resulting governing equations using numerical and asymptotic methods to cover the whole range of L^*/L, from a very long fin, $L^*/L \ll 1$, to a short fin, $L^*/L \gg 1$. They showed that a self-similar solution exists for a sufficiently long fin.

The present paper considers the same problem described in Ref. 10, but with the temperature at the top of the fin oscillating around a mean value above the ambient temperature of the fluid far from the fin. The transient problem introduces three additional nondimensional parameters, γ, Fourier number Fo, and A. Here γ is the ratio of the amplitude of the thermal oscillation to the temperature difference between the mean temperature at the top of the fin and the ambient temperature. The Fourier number Fo is the square of the ratio of the oscillatory thermal penetration length (L_ω to be given) to the steady thermal penetration length L^*: $Fo = (L_\omega/L^*)^2$. Finally, A is the ratio of the residence time of the fluid in the boundary layer around the fin to the heat conduction time along the fin. Only the important case of very long fins satisfying $L \gg L^*$ is discussed in what follows, which makes irrelevant the actual length of the fin. In this work, perturbation and numerical methods are employed, together with the boundary-layer approximation for the fluid.

II. Order of Magnitude Estimates

The physical problem under study is shown in Fig. 1. A vertical fin of length L, thickness $2H \ll L$, and infinite width is immersed in a fluid with temperature T_∞, which is at rest far from the fin. The top of the fin is maintained at a temperature, which is higher than T_∞ and oscillates harmonically with time in the form $T_u = T_0 + \Delta T \sin \omega t$, with $T_0 > T_\infty$. This induces a heat flux from the fin to the fluid, which gives rise to an upward natural convection flow around the fin.

Consider first the stationary flow, $\Delta T = 0$, around an infinitely long fin, $L \to \infty$. Because of the heat transfer to the surrounding fluid, the temperature of the fin decreases downward from its top, decaying toward the ambient temperature of the fluid in a thermal penetration region whose characteristic length L^* can be estimated from the balance of heat transfer to the fluid and heat conduction along the fin. When it is assumed that the Rayleigh number $Ra^* = g\beta(T_0 - T_\infty)L^{*3}/\alpha\nu \gg 1$ (where β, α, and ν are the thermal expansion coefficient, thermal diffusivity, and kinematic viscosity of the fluid), the flow around the fin is confined to a natural convection boundary layer of characteristic thickness $\delta \sim L^*/Ra^{*1/4}$, where the characteristic longitudinal velocity of the fluid is of order $u_c \sim \alpha Ra^{*1/2}/L^*$. These well-known estimates, for example, by Bejan,[11] follow from the order-of-magnitude balances of vertical convection and horizontal conduction across the boundary layer $[u_c(T_0 - T_\infty)/L^* \sim \alpha(T_0 - T_\infty)/\delta^2]$ and of buoyancy and viscous forces $[g\beta(T_0 - T_\infty) \sim \nu u_c/\delta^2]$. The total heat lost by the fin per unit time by conduction to the fluid, for example, Q, is of the order of $L^*\lambda(T_0 - T_\infty)/\delta$, where λ is the thermal conductivity of the fluid, whereas the heat conducted along the fin is of order $H\lambda_w(T_0 - T_\infty)/L^*$, where λ_w is the thermal conductivity of the fin. The balance of these two fluxes yields

$$L^* = H\left[(\lambda_w/\lambda)^{\frac{4}{7}} \Big/ Ra_H^{\frac{1}{7}}\right] \tag{1}$$

where $Ra_H = g\beta(T_0 - T_\infty)H^3/\alpha\nu$ is the Rayleigh number based on the half-thickness of the fin, which is not necessarily large compared with unity. On the basis of this estimate of the thermal penetration length, finite length fins can be classified as long, if $L \gg L^*$, or short, if $L \ll L^*$. In the first case, which is the subject of this paper, the actual length of the fin is irrelevant and the overall stationary Nusselt number, or nondimensional measure of the total heat Q evacuated by the fin per unit time is, from the earlier estimates,

$$Nu = Q/\lambda(T_0 - T_\infty) = \mathcal{O}(Ra^{*\frac{1}{4}}) = \mathcal{O}\left[(\lambda_w/\lambda)^{\frac{3}{7}} Ra_H^{\frac{1}{7}}\right] \tag{2}$$

The temperature variation across the fin must be estimated to ascertain the conditions of validity of the thermally thin-fin approximation, which will be used in what follows. When ΔT_{wh} is the characteristic temperature variation across the fin, the condition that the heat flux entering the fluid should come from the solid implies $\lambda(T_0 - T_\infty)/\delta \sim \lambda_w \Delta T_{wh}/H$, or, with use of the earlier estimate of δ,

$$\Delta T_{wh}/(T_0 - T_\infty) \sim (\lambda/\lambda_w)^{\frac{8}{7}} Ra_H^{\frac{2}{7}} \sim (H/L^*)^2 \tag{3}$$

for all but very short fins. Therefore, the thermally thin approximation $[\Delta T_{wh} \ll (T_0 - T_\infty)]$ is valid whenever the thickness of the fin is small compared with the thermal penetration length, as could have been advanced. This condition is satisfied when $\lambda_w \gg \lambda Ra_H^{1/4}$, or in terms of Ra^*, when $Ra^* \ll (\lambda_w/\lambda)^4$. Within this approximation, the temperature of the fin depends, in a first approximation, only on the distance x along the fin and on the time.

The time it takes to establish a stationary regime when the temperature of the top of the fin is suddenly raised from T_∞ to $T_0 > T_\infty$ is the largest between the conduction time in the solid, $t_c = L^{*2}/\alpha_w$, and the residence time of the fluid in the boundary layer, $t_r = L^*/u_c$. Here $\alpha_w = \lambda_w/\rho_w c_w$ is the thermal diffusivity of the fin material. The ratio

$$A = t_r/t_c = (\alpha_w/\alpha) \Big/ Ra^{*\frac{1}{2}} \tag{4}$$

measures the importance of nonstationary effects in the boundary layer during this transient.

A third characteristic time, equal to $1/\omega$, is introduced by the oscillation of the temperature of the top of the fin when $\Delta T \neq 0$. The ratio of this time to t_c is the Fourier number

$$Fo = (1/\omega)/t_c = \alpha_w \Big/ L^{*2}\omega \tag{5}$$

The ratio $A/Fo = t_r\omega$ measures the importance of nonstationary effects in the boundary layer. The flow in the boundary layer is quasi stationary during the oscillatory process if $Fo \gg A$. If $Fo \gg \max(1, A)$, then the whole process is quasi stationary, both in the fluid and in the solid, and the results of Ref. 10 can be applied replacing T_0 by the instantaneous value of the top fin temperature T_u.

The opposite case of $Fo \ll 1$ corresponds to the limit of high frequencies. The Fourier number can be interpreted as the square of the ratio of the oscillatory conduction penetration length $L_\omega = (\alpha_w/\omega)^{1/2}$ to L^*, so that $L_\omega \ll L^*$ in this limit. An important feature of the high-frequency limit is that heat transfer to the fluid ceases to play a role in the oscillatory process. This is because temperature oscillations in the fluid extend only to a sublayer of characteristic thickness $\delta_\omega = \delta \max[Fo^{1/6}, (Fo/A)^{1/2}]$, where δ is the thickness of the stationary boundary layer estimated earlier, leading to a characteristic oscillatory heat transfer rate $L_\omega\lambda\Delta T/\delta_\omega$, which is small compared with the characteristic flux along the fin,

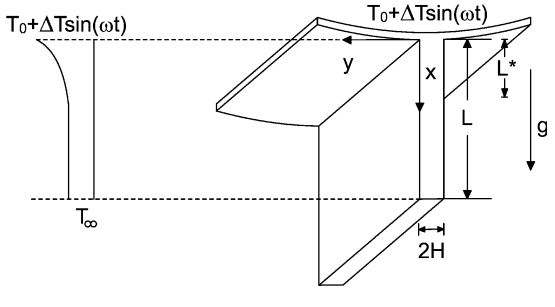

Fig. 1 Schematics of studied heat transfer configuration.

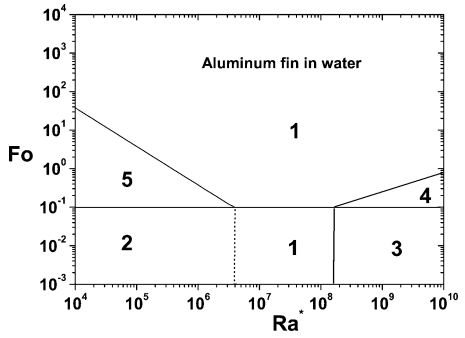

Fig. 2 Validity regions of quasi-steady and thermally thin-fin approximations in Rayleigh number Ra^* and Fourier number Fo parametric space.

$H\lambda_w \Delta T/L_\omega$, for any $A \ll 1/Fo$. The earlier estimate of δ_ω follows from the balance of convection and conduction in the oscillatory sublayer, $\rho c u_\omega \Delta T/L_\omega \sim \lambda \Delta T/\delta_\omega^2$, where the characteristic velocity is $u_\omega = u_c(\delta_\omega/\delta)$, or from the balance of heat accumulation and conduction, $\rho c \omega \Delta T \sim \lambda \Delta T/\delta_\omega^2$. The first balance applies when the oscillatory sublayer is quasi stationary ($A \ll Fo^{2/3}$) and the second balance applies in the opposite case.

Figure 2 is a schematic of the different regimes in the (Rayleigh number Ra^*, Fourier number Fo) plane for a set of parameter values corresponding to a fin of aluminum in water. The thermally thin approximation for heat conduction in the solid, $Ra^* \ll (\lambda_w/\lambda)^4$, is applicable at the left of the vertical solid line in Fig. 2. The high-frequency regime, in which the effect of the fluid on the oscillatory process is negligible, extends to the region below the horizontal line. The quasi stationary approximation for the flow in the boundary layer ($A/Fo \ll 1$) can be used above the inclined line at the left of Fig. 2. Therefore, the quasi stationary boundary-layer and thermally thin approximations are valid in region 1, whereas non-stationary effects in the boundary layer are important in region 2. These effects would still be important in part of region 3, but the whole analysis of the fluid may be dispensed within this region. The thermally thin approximation fails in region 4; however this is of no consequence for the oscillatory part of the solution in the lower right rectangle of Fig. 2 because the oscillatory heat transfer to-the fluid is negligible there. Finally, the quasi-steady approximation is not valid in region 5.

If water is replaced by air as a coolant, then the inclined and vertical lines of Fig. 2 shift to the left and to the right, respectively, enlarging region 1. The quasi-stationary and thermally thin approximations are valid virtually everywhere in this latter case.

III. Formulation

When the thermally thin-fin approximation (valid everywhere excluding region 4) is employed, the transient heat transfer problem can be studied using the following nondimensional variables:

$$\theta = \frac{T(x,y,t) - T_\infty}{T_0 - T_\infty}, \qquad \theta_w = \frac{T_w(x,t) - T_\infty}{T_0 - T_\infty}$$

$$U = \frac{L^*}{\alpha Ra^{*\frac{1}{2}} \sigma_0^{\frac{1}{2}}} u, \qquad V = \frac{\sigma_0^{\frac{1}{4}} L^*}{\alpha Ra^{*\frac{1}{4}}} v$$

$$\zeta = 1 + \frac{x}{\sigma_0 L^*}, \qquad Y = \frac{y}{\sigma_0^{\frac{1}{4}} L^*} Ra^{*\frac{1}{4}}, \qquad \tau = \omega t \tag{6}$$

where x is the vertical distance measured downward from the top of the fin, $x = 0$; y is the horizontal distance from the surface of the fin, positive in the fluid; and σ_0 is a function of Prandtl number Pr introduced for convenience (to be discussed). When the boundary-layer approximation is used, for large values of the Rayleigh number Ra^* compared with unity, the nondimensional governing equations (mass conservation, fluid momentum, and fluid and solid energy) are

$$\frac{\partial U}{\partial \zeta} + \frac{\partial V}{\partial Y} = 0 \tag{7}$$

$$\frac{\sigma_0^{\frac{1}{2}} A}{Fo} \frac{\partial U}{\partial \tau} + \frac{1}{Pr}\left(U \frac{\partial U}{\partial \zeta} + V \frac{\partial U}{\partial Y} \right) = -\theta + \frac{\partial^2 U}{\partial Y^2} \tag{8}$$

$$\frac{\sigma_0^{\frac{1}{2}} A}{Fo} \frac{\partial \theta}{\partial \tau} + U \frac{\partial \theta}{\partial \zeta} + V \frac{\partial \theta}{\partial Y} = \frac{\partial^2 \theta}{\partial Y^2} \tag{9}$$

$$\frac{\sigma_0^2}{Fo} \frac{\partial \theta_w}{\partial \tau} = \frac{\partial^2 \theta_w}{\partial \zeta^2} + \sigma_0^{\frac{7}{4}} \frac{\partial \theta}{\partial Y}\bigg|_{Y=0} \tag{10}$$

Equations (7–10) have to be solved with the following boundary conditions:

$$U = V = \theta - \theta_w = 0 \qquad \text{at} \qquad Y = 0 \tag{11}$$

$$U = \theta = 0 \qquad \text{for} \qquad Y \to \infty \tag{12}$$

$$\theta_w = 1 + \gamma \sin \tau \qquad \text{at} \qquad \zeta = 1$$

$$\theta_w = 0 \qquad \text{for} \qquad \zeta \to \infty \tag{13}$$

where $\gamma = \Delta T/(T_0 - T_\infty)$. The initial conditions are of no importance in the determination of the periodic solutions because we are looking for the time-periodic solutions.

To solve the nonlinear set of Eqs. (7–13), it is convenient to introduce the following transformed variables:

$$\theta = \theta_w(\zeta, \tau)\phi(\zeta, \xi, \tau), \qquad \xi = Y/\zeta^2$$

$$U = \frac{1}{\zeta^3} \frac{\partial h(\zeta, \xi, \tau)}{\partial \xi}$$

$$V = -\frac{1}{\zeta} \frac{\partial h(\zeta, \xi, \tau)}{\partial \zeta} + \frac{1}{\zeta^2}\left[h(\zeta, \xi, \tau) + 2\xi \frac{\partial h(\zeta, \xi, \tau)}{\partial \xi} \right] \tag{14}$$

In this form, the transformed governing equations reduce to

$$\frac{\sigma_0^{\frac{1}{2}} A \zeta^4}{Fo} \frac{\partial}{\partial \tau}\left(\frac{\partial h}{\partial \xi} \right) + \frac{1}{Pr}\left[h \frac{\partial^2 h}{\partial \xi^2} - 3\left(\frac{\partial h}{\partial \xi} \right)^2 + \zeta\left(\frac{\partial h}{\partial \xi} \frac{\partial^2 h}{\partial \zeta \partial \xi} - \frac{\partial h}{\partial \zeta} \frac{\partial^2 h}{\partial \xi^2} \right) \right] = -\theta_w \zeta^7 \phi + \frac{\partial^3 h}{\partial \xi^3} \tag{15}$$

$$\frac{\sigma_0^{\frac{1}{2}} A \zeta^4}{Fo \theta_w} \frac{\partial (\theta_w \phi)}{\partial \tau} + h \frac{\partial \phi}{\partial \xi} + \frac{\zeta}{\theta_w} \frac{\partial \theta_w}{\partial \zeta} \phi \frac{\partial h}{\partial \xi} + \zeta\left(\frac{\partial \phi}{\partial \zeta} \frac{\partial h}{\partial \xi} - \frac{\partial \phi}{\partial \xi} \frac{\partial h}{\partial \zeta} \right) = \frac{\partial^2 \phi}{\partial \xi^2} \tag{16}$$

$$\frac{\sigma_0^2}{Fo} \frac{\partial \theta_w}{\partial \tau} = \frac{\partial^2 \theta_w}{\partial \zeta^2} + \sigma_0^{\frac{7}{4}} \frac{\theta_w}{\zeta^2} \frac{\partial \phi}{\partial \xi}\bigg|_{\xi=0} \tag{17}$$

When the new variables are used, boundary conditions (11) and (12) are now written as

$$\frac{\partial h}{\partial \xi} = h = \phi - 1 = 0 \qquad \text{at} \qquad \xi = 0$$

$$\frac{\partial h}{\partial \xi} = \phi = 0 \qquad \text{for} \qquad \xi \to \infty \tag{18}$$

When the present formulation is used, the reduced nondimensional heat transfer or Nusselt number takes the form

$$Nu^* = \frac{Nu}{Ra^{*\frac{1}{4}}} = \frac{Q}{\lambda(T_0 - T_\infty) Ra^{*\frac{1}{4}}} = -\frac{1}{\sigma_0} \frac{\partial \theta_w}{\partial \zeta}\bigg|_{\zeta=1} \tag{19}$$

Problems (13) and (15–18) have a stationary solution when $\gamma = 0$. This solution, which has been computed elsewhere,[10] has $\theta_{ss} = 1/\zeta^7$ when the factor $\sigma_0(Pr)$ is chosen properly because $\sigma_0 = (-56/\mathrm{d}\phi_0/\mathrm{d}\xi|_{\xi=0})^{4/7}$ to satisfy the stationary form of Eq. (17). Here $\phi_0(\xi, Pr)$ has to be obtained from the self-similar solution of Eqs. (15) and (16),

$$\frac{1}{Pr}\left[h_0\frac{\mathrm{d}^2h_0}{\mathrm{d}\xi^2} - 3\left(\frac{\mathrm{d}h_0}{\mathrm{d}\xi}\right)^2\right] = -\phi_0 + \frac{\mathrm{d}^3h_0}{\mathrm{d}\xi^3} \tag{20}$$

$$h_0\frac{\mathrm{d}\phi_0}{\mathrm{d}\xi} - 7\phi_0\frac{\mathrm{d}h_0}{\mathrm{d}\xi} = \frac{\mathrm{d}^2\phi_0}{\mathrm{d}\xi^2} \tag{21}$$

to be solved with the boundary conditions $h_0 = \mathrm{d}h_0/\mathrm{d}\xi = \phi_0 - 1 = 0$ at $\xi = 0$ and $\mathrm{d}h_0/\mathrm{d}\xi = \phi_0 = 0$ for $\xi \to \infty$.

IV. Asymptotic Solution for $\gamma \ll 1$

A solution of Eqs. (15–18) and (13) can be obtained for values of γ small compared with unity by assuming the following expansions:

$$\begin{aligned}\theta_w(\zeta,\tau) &= (1/\zeta^7)[1+\gamma\varphi(\zeta,\tau)] + \mathcal{O}(\gamma^2)\\ h(\zeta,\xi,\tau) &= h_0(\xi) + \gamma h_1(\zeta,\xi,\tau) + \mathcal{O}(\gamma^2)\\ \phi(\zeta,\xi,\tau) &= \phi_0(\xi) + \gamma\phi_1(\zeta,\xi,\tau) + \mathcal{O}(\gamma^2)\end{aligned} \tag{22}$$

Here $\varphi(\zeta,\tau)$, $\phi_1(\zeta,\xi,\tau)$, and $h_1(\zeta,\xi,\tau)$ are the imaginary parts of the complex functions

$$\begin{Bmatrix}\tilde{\varphi}(\zeta,\tau)\\ \tilde{\phi}_1(\zeta,\xi,\tau)\\ \tilde{h}_1(\zeta,\xi,\tau)\end{Bmatrix} = \begin{Bmatrix}\Psi(\zeta)\\ \Phi_1(\zeta,\xi)\\ H_1(\zeta,\xi)\end{Bmatrix}\exp(i\tau) \tag{23}$$

where $i = \sqrt{-1}$ is the imaginary unit. That is, $\varphi(\zeta,\tau) = \Psi_r(\zeta)\sin(\tau) + \Psi_i(\zeta)\cos(\tau)$, where $\Psi_r(\zeta)$ and $\Psi_i(\zeta)$ are the real and imaginary parts of the complex function $\Psi(\zeta)$, and similarly for ϕ_1 and h_1. Carrying this to Eq. (17), we obtain

$$\frac{\mathrm{d}^2\Psi}{\partial\zeta^2} - \frac{14}{\zeta}\frac{\mathrm{d}\Psi}{\partial\zeta} + \frac{\sigma_0^{\frac{7}{4}}}{\zeta^2}\frac{\partial\Phi_1}{\partial\xi}\bigg|_0 = \frac{\sigma_0^2}{Fo}i\Psi \tag{24}$$

to be solved with the boundary conditions $\Psi(1) = 1 + i0$ and $\Psi(\infty) = 0 + i0$. When the linearized versions of Eqs. (15) and (16) are used, the resulting equations for the complex functions $\Phi_1(\zeta,\xi)$ and $H_1(\zeta,\xi)$ take the form

$$\begin{aligned}i\frac{\sigma_0^{\frac{1}{2}}A}{Fo}\zeta^4\frac{\partial H_1}{\partial\xi} + \frac{1}{Pr}\Bigg[&-6\frac{\mathrm{d}h_0}{\mathrm{d}\xi}\frac{\partial H_1}{\partial\xi} + h_0\frac{\partial^2H_1}{\partial\xi^2} + H_1\frac{\mathrm{d}^2h_0}{\mathrm{d}\xi^2}\\ &+\zeta\left(\frac{\mathrm{d}h_0}{\mathrm{d}\xi}\frac{\partial^2H_1}{\partial\zeta\partial\xi} - \frac{\partial H_1}{\partial\zeta}\frac{\mathrm{d}^2h_0}{\mathrm{d}\xi^2}\right)\Bigg] = -\Phi_1 - \Psi\phi_0 + \frac{\partial^3H_1}{\partial\xi^3}\end{aligned} \tag{25}$$

$$\begin{aligned}i\frac{\sigma_0^{\frac{1}{2}}A}{Fo}\zeta^4(\phi_0\Psi + \Phi_1) - 7\phi_0\frac{\partial H_1}{\partial\xi} - 7\Phi_1\frac{\mathrm{d}h_0}{\mathrm{d}\xi} + h_0\frac{\partial\Phi_1}{\partial\xi} + H_1\frac{\mathrm{d}\phi_0}{\mathrm{d}\xi}\\ +\zeta\phi_0\frac{\mathrm{d}\Psi}{\mathrm{d}\zeta}\frac{\mathrm{d}h_0}{\mathrm{d}\xi} + \zeta\left(\frac{\mathrm{d}h_0}{\mathrm{d}\xi}\frac{\partial\Phi_1}{\partial\zeta} - \frac{\partial H_1}{\partial\zeta}\frac{\mathrm{d}\phi_0}{\mathrm{d}\xi}\right) = \frac{\partial^2\Phi_1}{\partial\xi^2}\end{aligned} \tag{26}$$

The associated boundary conditions for Eqs. (25) and (26) can be written as

$$\begin{aligned}H_1|_{\zeta\to\infty} = \Phi_1|_{\zeta\to\infty} = H_1|_{\xi=0} = \Phi_1|_{\xi=0} = \frac{\partial H_1}{\partial\xi}\bigg|_{\xi=0}\\ = \frac{\partial H_1}{\partial\xi}\bigg|_{\xi\to\infty} = \Phi_1|_{\xi\to\infty} = 0 + i0\end{aligned}$$

The nondimensional heat flux or Nusselt number at the top of the fin is given by

$$Nu^* = -\frac{1}{\sigma_0}\frac{\partial\theta_w}{\partial\zeta}\bigg|_{\zeta=1} = Nu_0^* + \gamma Nu_1^* + \mathcal{O}(\gamma^2) \tag{27}$$

where $Nu_0^* = 7/\sigma_0$ and $Nu_1^* = [7\varphi(1,\tau) - \partial\varphi/\partial\zeta|_{\zeta=1}]/\sigma_0$. The corresponding value of Nusselt number Nu_1^* in this case is given by

$$Nu_1^* = \frac{1}{\sigma_0}\left[7 - \frac{\mathrm{d}\Psi_r}{\mathrm{d}\zeta}\bigg|_{\zeta=1}\right]\sin(\tau) - \frac{1}{\sigma_0}\frac{\mathrm{d}\Psi_i}{\mathrm{d}\zeta}\bigg|_{\zeta=1}\cos(\tau) \tag{28}$$

and its rms is then

$$\mathrm{rms}\{Nu_1^*\} = \left[\left(7 - \frac{\mathrm{d}\Psi_r}{\mathrm{d}\zeta}\bigg|_{\zeta=1}\right)^2 + \left(\frac{\mathrm{d}\Psi_i}{\mathrm{d}\zeta}\bigg|_{\zeta=1}\right)^2\right]^{\frac{1}{2}}\Big/\sqrt{2}\sigma_0 \tag{29}$$

For large values of Fourier number, $Fo \gg 1$, the quasi-steady approximation for the fin can be employed, giving $Nu_1^* = 35\sin(\tau)/4\sigma_0$. The rms of Nusselt number Nu_1^* is then $\mathrm{rms}\{Nu_1^*\} = 35/(4\sqrt{2}\sigma_0) = 6.1872/\sigma_0$.

On the other hand, for very small values of the Fourier number compared with unity (fast thermal oscillations), the longitudinal nondimensional coordinate must be rescaled in Eq. (24) with $\hat{\zeta} = (\zeta - 1)\sigma_0/Fo^{1/2}$, resulting in

$$\frac{\mathrm{d}^2\Psi}{\mathrm{d}\hat{\zeta}^2} - \frac{14Fo^{\frac{1}{2}}}{\sigma_0}\frac{\mathrm{d}\Psi}{\mathrm{d}\hat{\zeta}} + \frac{Fo}{\sigma_0^2}\frac{\partial\Phi_1}{\partial\xi}\bigg|_0 = i\Psi \tag{30}$$

The solution up to terms of order Fourier number $Fo^{1/2}$ is given by

$$\begin{aligned}\varphi(\hat{\zeta},\tau) = \exp\left\{-\left[1/\sqrt{2} - 7\left(Fo^{\frac{1}{2}}/\sigma_0\right)\right]\hat{\zeta}\right\}\\ \times\left[\cos\left(\hat{\zeta}/\sqrt{2}\right)\sin(\tau) - \sin\left(\hat{\zeta}/\sqrt{2}\right)\cos(\tau)\right] + \mathcal{O}(Fo)\end{aligned} \tag{31}$$

The first-order correction of the Nusselt number is then

$$Nu_1^* = \frac{7\varphi(0,\tau)}{\sigma_0} - \frac{1}{Fo^{\frac{1}{2}}}\frac{\partial\varphi}{\partial\hat{\zeta}}\bigg|_{\hat{\zeta}=0} = \frac{1}{\sqrt{2Fo}}[\cos(\tau) + \sin(\tau)] \tag{32}$$

The rms value of Nusselt number Nu_1^* is then

$$\mathrm{rms}\{\mathrm{Nu}_1^*\} = 1/\sqrt{2Fo} \qquad \text{for} \qquad Fo \to 0 \tag{33}$$

In this asymptotic limit, the first-order solution for the Nusselt number does not depend on σ_0, which means that is independent of the Prandtl number. Only the heat conduction along the fin determines the transient heat transfer process in this limit.

V. Numerical Solutions

Equations (15–17) with boundary conditions (13) and (18) have been numerically solved for different values of Fourier number Fo, A, Prandtl number Pr, and γ. A maximum value $\zeta_{\max}$ of ζ must be chosen in these computations that should be sufficiently large for the solution not to depend on it. It turns out that the minimum required $\zeta_{\max}$ is a strong function of the Fourier number. In our computations, it ranges from $\zeta_{\max} = 4$ for $Fo = 0.1$ to $\zeta_{\max} = 15$ for $Fo = 10$. These values were large enough not to be reached by the oscillatory thermal perturbation. The employed mesh size was 2000 points in the longitudinal direction ($\Delta\zeta = 0.0015$–0.007), 2001 points in the transverse direction ($\Delta\xi = 0.005$), and $\Delta\tau = 0.01$. At time equal zero, the temperature profile was set equal to the steady profile $\theta_w = 1/\zeta^7$, and $h_0(\xi)$ and $\phi_0(\xi)$ were obtained by solving Eqs. (20) and (21) with their corresponding boundary conditions. Starting from this initial profiles for $h(\zeta,\xi,\tau)$ and $\phi(\zeta,\xi,\tau)$, Eq. (17) was integrated in time using central difference discretization and the classical Crank–Nicholson scheme. The nonlinear term was linearized using the first-order Taylor series expansion. The linear algebraic system of equations was solved using the tridiagonal matrix solver, and convergence was achieved using a relaxation factor. After the fin

temperature profile is updated, Eqs. (15) and (16) are numerically integrated by decomposing the momentum Eq. (15) in a first-order and a second-order differential equation and using a central difference discretization and the quasi-linearization technique for the nonlinear terms. Equations (15) and (16) are then parabolic in the ζ direction and are solved by a standard iterative method.

Consider first the solution for $A = 0$, corresponding to a quasi-steady boundary layer. Figure 3 shows the steady-state solution for $dh_0/d\xi$ (Fig. 3a), which is related to the longitudinal fluid velocity and ϕ_0 (Fig. 3b) as a function of ξ for different values of the Prandtl number. The nondimensional temperature gradient at the fin decreases slightly as the Prandtl number decreases, for small values of the Prandtl number. When the limiting case of $Pr \to \infty$ is considered, the boundary condition for h_0, $d^2h_0/d\xi^2 = 0$, replaces the boundary condition (18) for $\xi \to \infty$. The value of σ_0 is given in Fig. 4 as a function of the Prandtl number. For large values of Prandtl number Pr, $\sigma_0 \to 9.461$, whereas for very small values of the Prandtl number, $\sigma_0 \to 7.096/Pr^{1/7}$.

Figure 5 shows the nondimensional temperature perturbation $\varphi = (\theta_w \zeta^7 - 1)/\gamma$, obtained numerically after solving Eqs. (15–17)

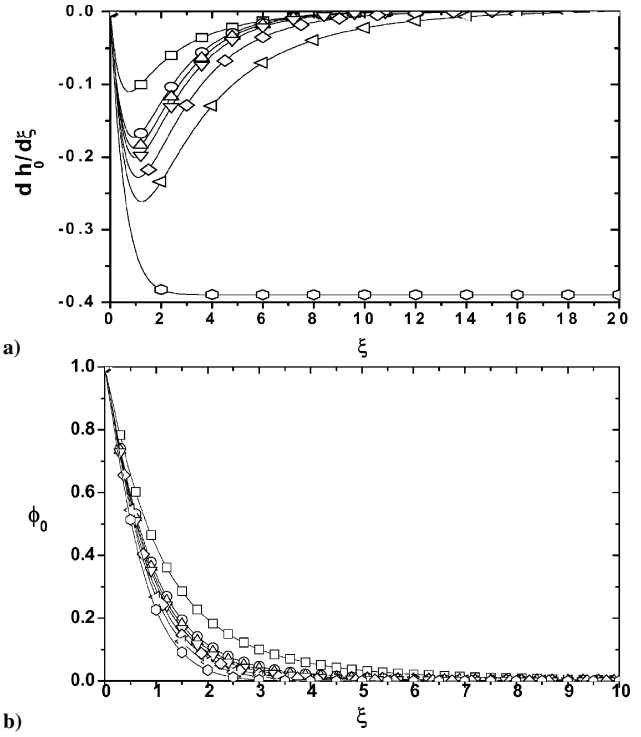

Fig. 3 Steady-state nondimensional longitudinal velocity and temperature profiles, obtained numerically as function of nondimensional coordinate ξ: a) $dh_0/d\xi$ and b) $\phi_0(\xi)$: □, $Pr = 0.1$; ○, $Pr = 0.5$; △, $Pr = 0.72$; ▽, $Pr = 1$; ◇, $Pr = 2$; ◁, $Pr = 5$; ▷, $Pr = 10$; and ⬡, $Pr = \infty$.

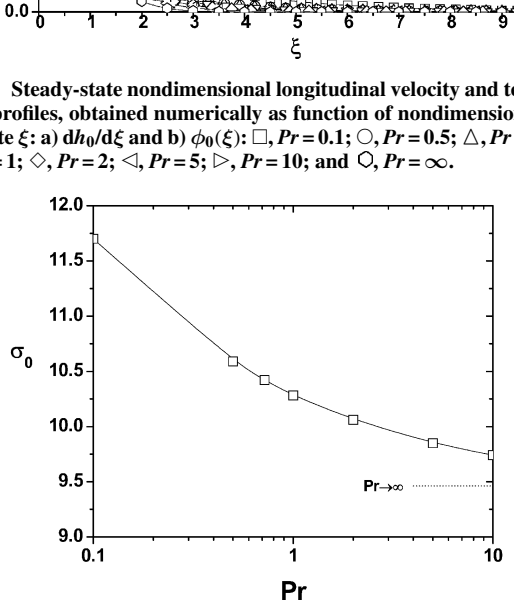

Fig. 4 Parameter σ_0 as function of Prandtl number.

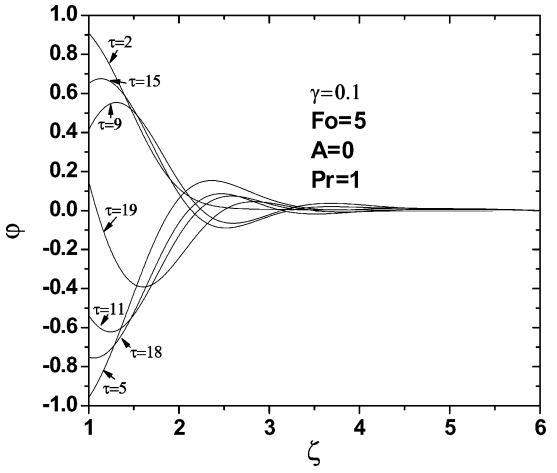

Fig. 5 Transient nondimensional temperature perturbation φ as function of nondimensional longitudinal coordinate obtained at different times: $Pr = 1$, $\gamma = 0.1$, $A = 0$, and $Fo = 5$.

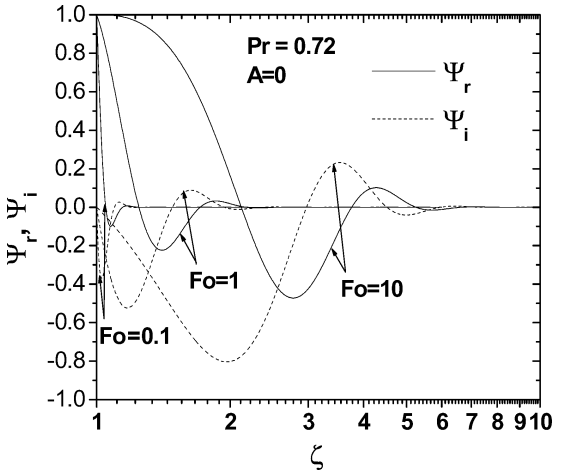

Fig. 6 Real and imaginary parts of function Ψ as function of nondimensional longitudinal coordinate; $A = 0$, $Pr = 0.72$, and three different Fourier numbers.

for a value of $\gamma = 0.1$, $Pr = 1$, and $Fo = 5$. The nondimensional temperature in the fin is plotted at different nondimensional times. The most important feature of Fig. 5 is the oscillatory penetration length, which is strongly influenced by the Fourier number. This penetration length is clearly shown in Fig. 6, where the real, $\Psi_r(\zeta)$, and the imaginary, $\Psi_i(\zeta)$, parts of the complex nondimensional temperature are plotted as functions of ζ, for three different values of the Fourier numbers, for $Pr = 0.72$. For values of the Fourier number $Fo = 10$, the oscillatory penetration length ζ is close to 10, whereas for small values of Fourier number, $Fo = 0.1$, the oscillatory penetration length is smaller than 1.5.

Figure 7 shows the rms value of oscillatory Nusselt number correction, $\text{rms}\{Nu_1^*\}$, as a function of the Fourier number, obtained by solving numerically Eqs. (15–17), with a value of $\gamma = 0.1$ (open symbols) and different values of the Prandtl number. The linear approximation with $\gamma \ll 1$, given by Eq. (24), is also plotted (lines). The behavior of the linear and nonlinear solutions is very similar. In Fig. 7, the asymptotic solution obtained for very small values of Fourier number compared with unity, given by Eq. (33), is also plotted. This asymptotic solution, which is in fact independent of the Prandtl number, gives very good results for values of $Fo < 0.1$.

In Fig. 8, the computed results for the $\text{rms}\{Nu_1^*\}$ are shown for a Prandtl number of $Pr = 0.72$ and different values of A, corresponding to nonstationary boundary layers of the flow surrounding the fin. The amplitude of the resulting oscillations for the Nusselt number increases with increasing values of A, for all possible numbers of the

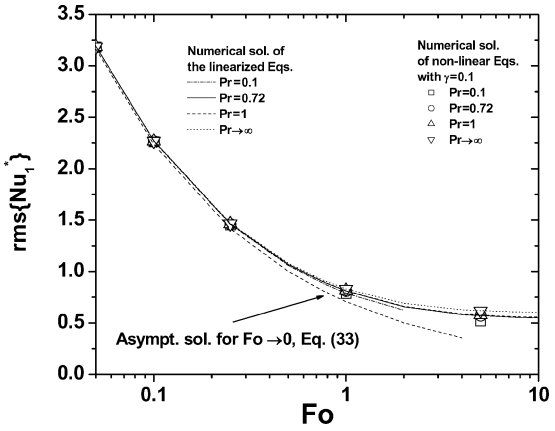

Fig. 7 Root mean square of first-order reduced Nusselt number as function of Fourier number for four different Prandtl numbers and $A = 0$.

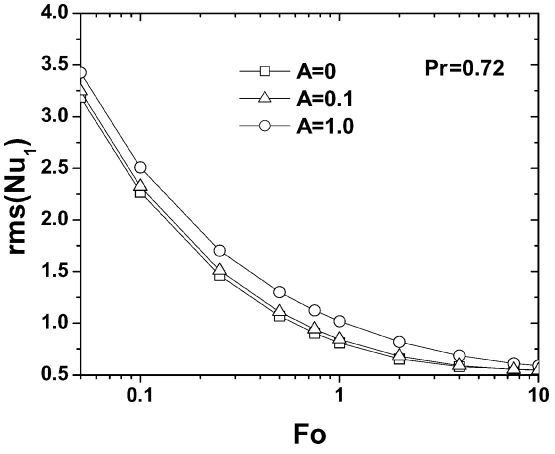

Fig. 8 Influence of nonstationary effects on rms of first-order reduced Nusselt number as function of Fourier number for $Pr = 0.72$.

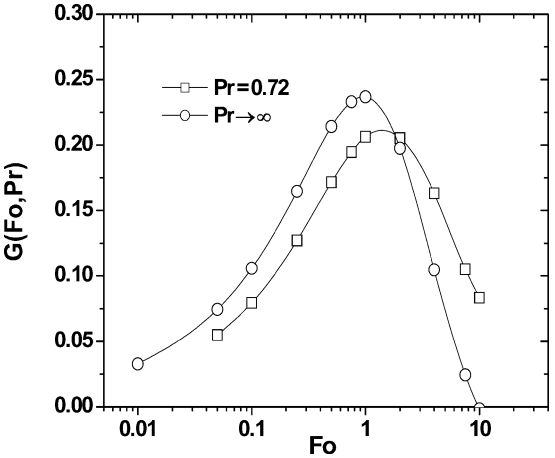

Fig. 9 Nondimensional function $G(Fo, Pr)$ as function of Fourier number for two Prandtl numbers.

Fourier number. A simple relationship of the influence of the nonstationary effects in the boundary layer on the oscillating correction of the Nusselt number can be written as

$$\mathrm{rms}\left\{Nu_1^*\right\} = [1 + AG(Fo, Pr)]\mathrm{rms}\left\{Nu_1^*\right\}_{A=0} \qquad (34)$$

where the subscript $A = 0$ corresponds to the quasi-steady solution for the boundary layer and $G(Fo, Pr)$ is shown in Fig. 9 for two values of $Pr = 0.72$ and $Pr \to \infty$. The maximum influence of the value of A on the Nusselt number corresponds to values of the

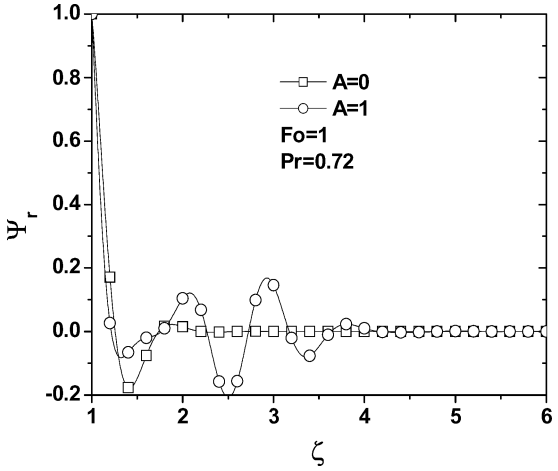

Fig. 10 Influence of nonstationary effects on real part of function Ψ, Ψ_r, as function of nondimensional longitudinal coordinate ζ, for $Pr = 0.72$ and $A = 0$ and $A = 1$.

Fourier numbers of order unity. Finally, to assess the nonstationary effects on the nondimensional temperature on the fin oscillating temperature, Fig. 10 shows the real part of the complex function Ψ plotted as a function of the nondimensional longitudinal coordinate ζ, for a value of $Fo = 1$, $Pr = 0.72$, and two different values of parameter A, that is, $A = 0$ and $A = 1$. The oscillating penetration length L_ω is shown to increase when the nonstationary effects in the fluid are considered in the analysis. The overall effect is to increase the amplitude of the resulting oscillating reduced Nusselt number for all possible values of the Fourier numbers.

VI. Conclusions

The transient conjugated heat transfer in a vertical fin has been studied using both analytical and numerical techniques. The temperature at the top of the fin oscillates around a mean temperature larger than the ambient temperature of the fluid far from the fin. This transient problem introduces three nondimensional parameters in addition to the steady-state process: γ, which relates the amplitude of the temperature due to the thermal oscillation to the steady-state temperature difference; the Fourier number $Fo = \alpha_w / L^{*2}\omega$, which relates the thermal penetration length of the transient process to the corresponding steady-state thermal penetration length; and A, which relates the characteristic residence time in the fluid to the characteristic diffusion time in the fin. The nonlinear problem has been solved using numerical techniques for any value of parameter γ. The results show that the linearized version of the governing equations seems to give excellent results for the oscillatory Nusselt number compared with the full nonlinear equations. The heat conduction along the fin determines the transient heat transfer problem in the limit of small Fourier numbers compared with unity. The results obtained by using the quasi-steady approximation for the fluid give always lower values of the amplitude of the oscillating heat transfer than those obtained when including the nonstationary effects.

References

[1]Merkin, J. H., and Pop, I., "Conjugate Free Convection on a Vertical Plate," *International Journal of Heat and Mass Transfer*, Vol. 39, No. 7, 1996, pp. 1527–1534.

[2]Vynnycky, M., and Kimura, S., "Conjugate Free Convection due to a Heated Vertical Plate," *International Journal of Heat and Mass Transfer*, Vol. 39, No. 5, 1996, pp. 1067–1080.

[3]Luna, E., Treviño, C., and Higuera, F. J., "Conjugate Natural Convection Heat Transfer Between Two Fluids Separated by an Horizontal Wall: Steady-State Analysis," *Heat and Mass Transfer*, Vol. 31, No. 5, 1996, pp. 353–358.

[4]Lock, G. S. H., and Gunn, J. C., "Laminar Free Convection from a Downward-Projecting Fin," *Journal of Heat Transfer*, Vol. 90, No. 1, 1968, pp. 63–70.

[5]Sparrow, E. M., and Acharya, S., "A Natural Convection Fin with a Solution-Determined Nonmonotonically Varying Heat Transfer Coefficient," *Journal of Heat Transfer*, Vol. 103, No. 2, 1981, pp. 218–225.

[6]Kuehn, T. H., Kwon, S. S., and Tolpadi, A. K., "Similarity Solution for Conjugate Natural Convection Heat Transfer from a Long Vertical Plate Fin," *International journal of Heat and Mass Transfer*, Vol. 26, No. 13, 1983, pp. 1718–1721.

[7]Himasekhar, K., "Integral Analysis of Conjugate Natural Convection Heat Transfer from a Long Vertical Fin," *International Journal of Heat and Mass Transfer*, Vol. 30, No. 2, 1987, pp. 201–203.

[8]Sarma, P. K., Subrahmanyam, T., and Dharma Rao, V., "Natural Convection from a Vertical Heat-Generating Fin—A Conjugate Problem," *Journal of Heat Transfer*, Vol. 110, No. 1, 1988, pp. 99–102.

[9]Mobedi, M., Saidi, A., and Sunden, B., "Computation of Conjugate Natural Convection Heat Transfer from a Rectangular Fin on a Partially Heated Horizontal Base," *Heat and Mass Transfer*, Vol. 33, No. 3, 1998, pp. 333–336.

[10]Treviño, C., Luna, E., Méndez, F., and Higuera, F. J., "Natural Convective Conjugate Cooling Mechanism in Vertical Fins," *Journal of Thermophysics and Heat Transfer*, Vol. 17, No. 3, 2003, pp. 396–401.

[11]Bejan, A., *Heat Transfer*, Wiley, New York, 1993, pp. 161–163.